

## Phase composition of stainless steel subjected to ultrasonic nanocrystal surface modification with different processing density

© Denis A. Polonyankin<sup>a</sup>✉, Alexey A. Fedorov<sup>a</sup>, Tatyana M. Gomonyuk<sup>a,b</sup>

<sup>a</sup> Omsk State Technical University, 11, Mira Av., Omsk, 644050, Russian Federation,

<sup>b</sup> CJSC "Elekton", 17 DC, 150, Raduzhny, 600910, Russian Federation

✉ dapolonyankin@omgtu.tech

**Abstract:** Improving physical and mechanical properties of austenitic stainless steels (ASS) by methods of surface severe plastic deformation (SSPD) is one of the key problematic topics in the field of surface engineering and nanocrystal materials. The complex nature of the structural states evolution under the conditions of SSPD restricts the possibilities of a specified nanostructuring of the type 18-10 ASS in a wide range of deformation impacts. The article presents the results of XRD and TEM analysis of AISI 321 near-surface layer after ultrasonic nanocrystal surface modification (UNSM) with different processing densities. The work used methods of X-ray diffraction analysis (XRD) and transmission electron microscopy (TEM) tested for examination of the structural and phase composition of the type 18-10 ASS subjected to UNSM. XRD and TEM indicate a two-phase ( $\alpha' + \gamma$ ) composition of the near-surface layer of AISI 321 steel processed by UNSM. The XRD technique has established the functional dependencies of the martensite volume fraction from 1) the processing density and 2) the strain energy density, the approximation of which by linear regression equations is performed with reliability  $R^2 = 0.984$ . According to TEM data, the structure of the near-surface layer of AISI 321 stainless steel subjected to UNSM with the maximum processing density used ( $N = 9367 \text{ mm}^{-2}$ ) is represented by a significant amount of martensite in the form of lamellae with the width of less than 100 nm and a high dislocation density. The results of this work can be used to develop and optimize the UNSM processing modes of the 18-10 ASS produced by subtractive, additive and hybrid additive-subtractive manufacturing technologies.

**Keywords:** ultrasonic nanocrystal surface modification; AISI 321 stainless steel; processing density; strain energy density; phase composition; austenite; deformation-induced martensite; phase volume fraction; lamellae nanostructure.

**For citation:** Polonyankin DA, Fedorov AA, Gomonyuk TM. Phase composition of stainless steel subjected to ultrasonic nanocrystal surface modification with different processing density. *Journal of Advanced Materials and Technologies*. 2024;9(4):257-266. DOI: 10.17277/jamt.2024.04.pp.257-266

## Фазовый состав нержавеющей стали, подвергнутой ультразвуковому нанокристаллическому поверхностному модифицированию с различной плотностью обработки

© Д. А. Полонянкин<sup>a</sup>✉, А. А. Федоров<sup>a</sup>, Т. М. Гомонюк<sup>a,b</sup>

<sup>a</sup> Омский государственный технический университет,  
пр. Мира, 11, Омск, 644050, Российская Федерация,

<sup>b</sup> ЗАО «Электон», кв-л 17, 150, Радужный, 600910, Российская Федерация

✉ dapolonyankin@omgtu.tech

**Аннотация:** Повышение физико-механических свойств аустенитных нержавеющей сталей (АНС) методами интенсивного поверхностного пластического деформирования (ИППД) является одной из ключевых проблемных тематик в области инженерии поверхности и нанокристаллических материалов. Комплексный характер эволюции структурных состояний в условиях ИППД ограничивает возможности регламентированного наноструктурирования приповерхностного слоя АНС типа 18-10 в широком диапазоне деформационных воздействий. Представлены

результаты рентгенофазового анализа (РФА) и просвечивающей электронной микроскопии (ПЭМ) приповерхностного слоя стали 12X18H10T после ультразвукового нанокристаллического поверхностного модифицирования (УНПМ) с различной плотностью обработки. РФА и ПЭМ свидетельствуют о двухфазном ( $\alpha' + \gamma$ ) составе стали 12X18H10T, подвергнутой УНПМ. Методом РФА установлены функциональные зависимости объемной доли мартенситной фазы: 1) от плотности обработки; 2) энергии деформации, аппроксимация которых уравнениями линейной регрессии выполняется с достоверностью  $R^2 = 0,984$ . По данным ПЭМ, структура приповерхностного слоя стали 12X18H10T, подвергнутой УНПМ с максимальной используемой плотностью обработки ( $N = 9367 \text{ мм}^{-2}$ ), представлена значительным количеством мартенсита в форме ламелей шириной менее 100 нм и высокой плотностью дислокаций. Результаты данной работы могут использоваться для разработки и оптимизации технологических режимов УНПМ АНС типа 18-10, полученных субтрактивными, аддитивными и гибридными аддитивно-субтрактивными технологиями производства.

**Ключевые слова:** ультразвуковое нанокристаллическое поверхностное модифицирование; нержавеющая сталь 12X18H10T; плотность обработки; плотность энергии деформации; фазовый состав; аустенит; мартенсит деформации; объемная доля фаз; ламельная наноструктура.

**Для цитирования:** Polonyankin DA, Fedorov AA, Gomonyuk TM. Phase composition of stainless steel subjected to ultrasonic nanocrystal surface modification with different processing density. *Journal of Advanced Materials and Technologies*. 2024;9(4):257-266. DOI: 10.17277/jamt.2024.04.pp.257-266

## 1. Introduction

Austenitic chromium-nickel steels belong to the most common type of austenitic stainless steels (ASS), the relative share of which in the world market exceeds 80 % [1]. Among austenitic stainless steels the most demanded are steels of type 18-10, alloyed with ~18 % chromium and 8 to 12 % nickel, the advantages of which are machinability and ductility, while the disadvantages are relatively low strength properties (hardness, yield strength, fatigue strength). Titanium-stabilized ASS of type 18-10 (including AISI 321 steel) are used in the petrochemical industry [2, 3], in conventional [4] and alternative energy generation [2], as well as in the nuclear industry [5, 6] and biomedicine [7].

The use of 18-10 ASSs in subtractive manufacturing is combined with their utilization in additive printing technologies, which have become widespread in the aerospace industry as well as in mechanical engineering [8]. Modern arc [9] and beam [10, 11] 3D printing technologies provide the possibility of precision manufacturing of complex-shaped products from AISI 321 steel in a wide range of standard sizes. Depending on the type of energy impact, the form factor of the source material and the method of its feeding during printing, it is possible to evolve inhomogeneous structure and high residual stresses, defects in the form of pores and microcracks, the formation of  $\delta$ -ferrite [12], as well as large columnar grains [8], which cause anisotropy of ASS properties [13].

The main approach to eliminating the above-mentioned disadvantages of additive as well as traditional subtractive ASS production is a scientifically based selection of optimal technological

modes and post-processing operations [8, 13, 14], which ensure the formation of the required quality of the working surface, phase composition of the near-surface layer and residual stresses acting in it [15]. At the same time, due to the low carbon content, it is very difficult to increase the strength of 18-10 ASS by final heat treatment [8], in contrast to plastic deformation [5]. At present, the formation of a regulated structural-phase state and optimization of mechanical properties of ASS of type 18-10 is quite effectively realized by methods of surface severe plastic deformation (SSPD), including ultrasonic nanocrystal surface modification (UNSM).

UNSM is one of the most popular methods of SSPD of metals and alloys (including ASS type 18-10) and formation of gradient nanostructured near-surface layer in them, which corresponds to nanotechnologies realized according to the “top-down” approach [16, 17]. It is important to note that a direct analog of UNSM is the technology of ultrasonic impact treatment (UIT) [7, 18]. The range of processes involved in the UNSM includes: 1) fragmentation of the initial grains with the formation of nanoscale structural elements, 2) microdeformation of the lattice, 3) formation of defects of various types, 4) structural phase transformations [17], but is not limited to them. During the UNSM process, the processed material is subjected to deformation effects with a strain rate ranging from 0.5 to  $10^6 \text{ s}^{-1}$  [19], which contributes to the formation of residual compressive stresses [20].

One of the main variable parameters of UNSM modes is the number of tip strikes per unit area of the processed surface ( $N$ ) [21], also referred to as “strike density” [18]. It is important to note that the UNSM strike density is inversely proportional to the speed at

which the tip moves over the surface [22] (“scanning speed” [19]). As reported in [21], the higher the surface density of UNSM, the greater the depth and degree of refinement of polycrystalline grains in the near-surface layer of steel, and the faster its transition to a nanostructured state. In addition, increasing the intensity of UNSM processing contributes to a rise in the volume fraction of deformation-induced martensite (DIM) in 18-10 ASS [23]. At the same time, UNSM performed with a strike density exceeding a certain critical value promotes the formation of surface defects in the form of fatigue cracks [24]. Thus, the establishment of optimal parameters of UNSM modes, including the surface density of processing of ASS type 18-10, is an important scientific and technological problem.

As shown by the literature review, information on the structural phase composition of 18-10 ASS subjected to UNSM with different processing density and strain energy is extremely limited. Moreover, there are no relevant experimental studies available in the public domain for AISI 321 steel. This determines the relevance and practical significance of this work, the purpose of which is to determine the dependence of the phase composition (volume fraction of austenite and deformation-induced martensite) on the processing density and strain energy, as well as to analyze the peculiarities of the structure of the near surface layer of AISI 321 steel subjected to UNSM.

## 2. Materials and Methods

### 2.1. Materials and processing parameters

To perform the experimental part of the work, a metal bar with a radius of 12.75 mm in delivery condition, made of stainless steel grade AISI 321 was used. The content of the main chemical elements in the steel was: 0.12 % C, 18.64 % Cr, 10.1 % Ni and 0.54 % Ti. From the pre-turned bar ( $Ra \sim 2.2 \mu\text{m}$ ) was cut a shaft with the length of 150 mm. Then the shaft was processed by ultrasonic nanocrystal surface modification in different modes (given in Table 1), namely, with different speed ( $v$ ,  $\text{m}\cdot\text{min}^{-1}$ ) of

relative movement of the cylindrical surface of the shaft and the tip made of alloy VK8. UNSM was carried out on the unit consisting of the technological module DTM-07, magnetostrictive transducer PMS15A-18 and a waveguide with a spherical shaped indenter (tip) of diameter  $d = 6 \text{ mm}$ . During UNSM the following parameters of the processing mode were kept constant: 1) frequency of the ultrasonic generator ( $f = 18 \text{ kHz}$ ); 2) amplitude of the indenter oscillations ( $\xi_m = 0.05 \text{ mm}$ ); 3) force of pressing the ultrasonic tool to the processed surface (static load,  $F_{st} = 30 \text{ N}$ ); 4) longitudinal tool feed ( $s = 0.09 \text{ mm}\cdot\text{rev}^{-1}$ ).

In the case of tip machining of a cylindrical surface (shaft), the speed of their relative displacement  $v$  is determined through the radius ( $[r] = \text{m}$ ) and shaft rotation frequency ( $[n] = \text{rev}\cdot\text{s}^{-1}$ ) by the formula  $v = 2\pi r \cdot n$  ( $[v] = \text{m}\cdot\text{rev}\cdot\text{s}^{-1}$ ). Taking into account the frequency of ultrasonic vibrations of the tool ( $f$ , Hz), the radius and rotation frequency of the shaft, the strike density ( $[N] = \text{m}^{-2}$ ) during UNSM is calculated by the formula (1):

$$N = \frac{60 f}{v s} = \frac{60 f}{(2\pi r \cdot n) s}, \quad (1)$$

where  $[s] = \text{m}\cdot\text{rev}^{-1}$  is the longitudinal tool feed.

In turn, the strain energy density ( $E$ ) transferred to the near-surface layer during its processing by the indenter is estimated according to the formula (2) [19, 21, 25]:

$$E = \frac{F_{st} N \xi_m}{d}, \quad (2)$$

where  $[E] = \text{J}\cdot\text{m}^{-3}$ ,  $[F_{st}] = \text{N}$ ,  $[N] = \text{m}^{-2}$ ,  $[\xi_m] = \text{m}$ ,  $[d] = \text{m}$ .

It should be noted that, as a rule, the surface processing density is recalculated per square millimeter [21, 22], and the strain energy density is expressed in  $\text{J}\cdot\text{mm}^{-3}$  [25].

For clarity, the designations of the specimens subjected to UNSM with different surface processing densities will be used hereafter as presented in Table 1.

**Table 1.** UNSM modes, the relevant surface processing density and strain energy density

Specimen	$n$ , $\text{rev}\cdot\text{min}^{-1}$	$v$ , $\text{m}\cdot\text{min}^{-1}$	$N$ , $\text{mm}^{-2}$	$E$ , $\text{J}\cdot\text{mm}^{-3}$
N1	16	1,28	9367	2,34
N2	25	2,00	5995	1,50
N3	45	3,60	3330	0,83
N4	63	5,04	2379	0,59
N5	100	8,00	1499	0,37

## 2.2. Characterization techniques

XRD analysis of samples before and after UNSM with different processing densities was carried out using a Shimadzu Maxima XRD-7000 diffractometer equipped with a copper cathode X-ray tube ( $\lambda = 0.15406$  nm). Before XRD, which is universally used to identify the phase composition of 18-10 ASS, the diffractometer was adjusted according to the internal standard technique using silicon powder. For comparative analytical study of the phase composition of the samples, the diffractograms were recorded in the standard  $\theta$ - $2\theta$  mode using the following imaging parameters: voltage and current on the X-ray tube 50.0 kV and 40.0 mA, respectively, width of the divergence and receiving slits 1.0 deg and 0.3 mm, respectively, range and scanning speed  $2\theta = (30\div 100)$  deg and  $0.50$  deg $\cdot$ min $^{-1}$ , respectively. The “Basic Process” operation of the software “XRD-6100/7000 Ver.7.00: main” was used to process all the obtained diffractograms, providing the possibility of profile smoothing, background subtraction, separation of  $K\alpha_1$ - and  $K\alpha_2$ -lines, as well as correction of systematic errors. The transcription reports of the raw diffractograms contain information on the integral intensity of the reflexes, their full width at half maximum, and the corresponding diffraction angles and interplanar spacing. The volume fractions of austenite and deformation-induced martensite in the near-surface layer of UNSM-treated samples were estimated by analogy with [26] using the formula:

$$V_\gamma = \frac{1.4I_\gamma}{1.4I_\gamma + I_{\alpha'}}, \quad (3)$$

where  $I_\gamma, I_{\alpha'}$ ,  $V_\gamma$  and  $V_{\alpha'} = (1 - V_\gamma)$  are integral intensities of  $(111)\gamma$  and  $(110)\alpha'$  reflexes, as well as volume fractions of austenitic and martensitic phases, respectively. The strongest reflexes of austenitic  $(111)$  and martensitic  $(110)$  phases were additionally registered three times in the range of angles  $2\theta = (40\div 50)^\circ$  with the following statistical processing of the obtained integral intensity values according to the method of indirect reproducible measurements.

The structural features of the surface layer of AISI 321 steel after UNSM were studied by transmission electron microscopy (TEM) with an accelerating voltage of 120 kV on a Philips SM-12 device. The preparation of the foil samples for the TEM study was carried out using the Quanta 200 3D complex according to the standard technique of obtaining cross-sectional (normal) profiles with a

focused beam of gallium ions. The structural state of the N1 sample subjected to UNSM with the processing density  $N = 9367$  mm $^{-2}$  was studied by TEM.

## 3. Results and Discussion

Figure 1 demonstrates the diffractograms of AISI 321 stainless steel samples before and after UNSM with different processing densities. As Figure 1 shows, the diffractogram of the untreated sample corresponds to the FCC lattice of iron: the maxima in the region of diffraction angles  $43.6^\circ$ ,  $50.7^\circ$ ,  $74.5^\circ$ ,  $90.6^\circ$  and  $95.9^\circ$  are formed by the lattice planes of the  $\gamma$ -phase of iron (austenite). The composition of the near-surface layer of all UNSM-treated samples is biphasic and, in addition to austenite, is represented by deformation-induced martensite with a BCC lattice, which is confirmed by the presence of reflexes in the diffractograms in the region of angles  $44.5^\circ$ ,  $64.5^\circ$ ,  $81.8^\circ$  and  $98.4^\circ$  corresponding to the lattice planes of  $\alpha'$ -phase iron (martensite) [26, 27].

As the UNSM processing density increases, the diffractograms of AISI 321 steel samples (Figure 1) in the range of angles  $2\theta = (40\div 50)^\circ$  show a multidirectional change in the intensity of reflexes formed by the lattice planes  $(111)\gamma$  and  $(110)\alpha'$ , which correlates with the literature data, for example [28]. Figure 2 shows the corresponding dependences of the volume fraction of phases on the strain energy density (Fig. 2a) and surface processing density (Fig. 2b) of samples of AISI 321 steel by the UNSM method. The reliability of approximation by the linear regression equation is  $R^2 = 0.984$ .

Thus, UNSM ensures the formation of DIM in the near-surface layer of all samples of AISI 321 steel. The martensite volume fraction is in direct dependence on the strain energy density, as well as on the surface processing density. To interpret the obtained functional dependences, let us turn to the physical basis of ultrasonic nanocrystal surface modification. During UNSM, the kinetic energy of the tool's mechanical vibrations performed with ultrasonic frequency is converted into the energy of the tip impact on the treated surface. Accumulation and dissipation of the kinetic energy transferred from the tip to the ASS near-surface layer is accompanied by the appearance of elastic and plastic deformations in it, as well as local adiabatic heating [19].

Meanwhile, the fraction of the initial mechanical energy that is not converted into heat and used for plastic deformation is stored inside the treated material and is called accumulated or latent energy [29], as well as strain energy [30].

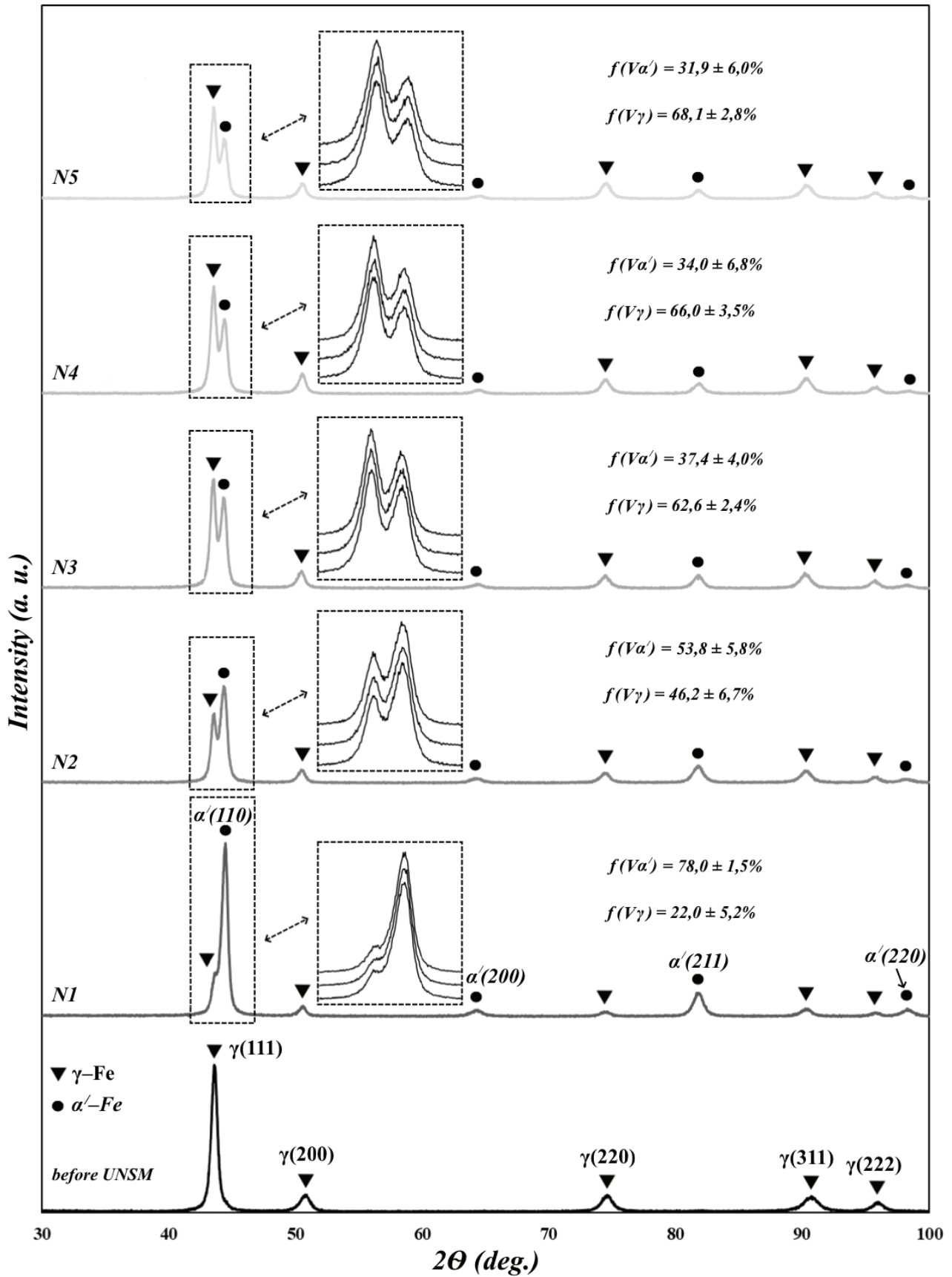


Fig. 1. Jointly presented XRD patterns of AISI 321 stainless steel before and after ultrasonic nanocrystal surface modification with different processing density

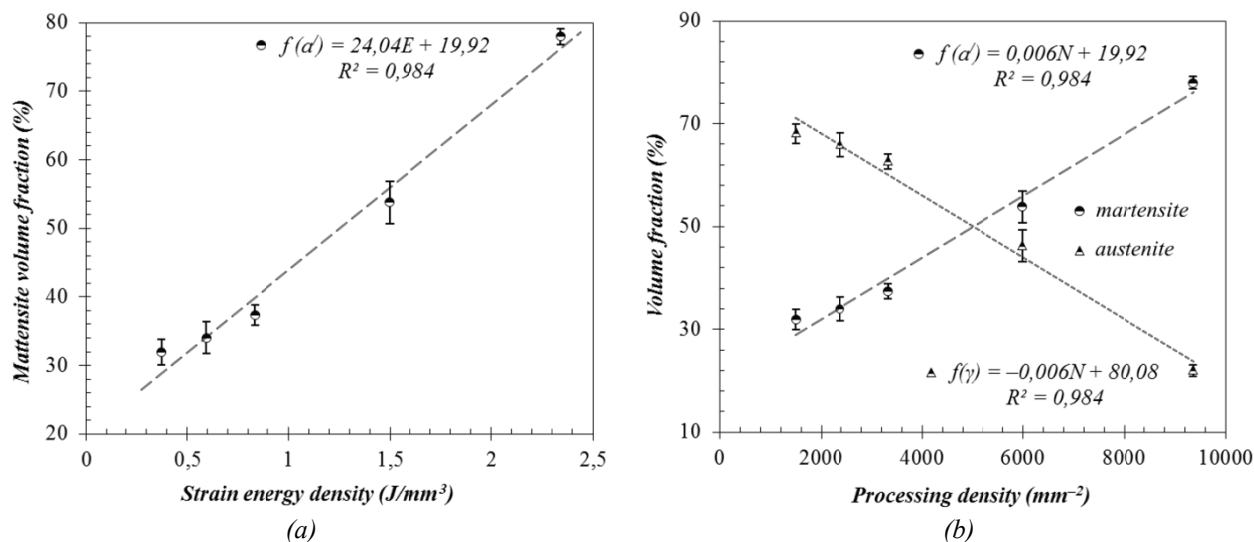


Fig. 2. Dependencies of austenite and martensite volume fractions in AISI 321 steel near-surface layer from (a) strain energy density and (b) processing density induced by UNSM

At the same time, as noted in [31], it is possible to neglect thermal losses during ultrasonic impact treatment and to consider strain hardening of AISI 304 steel (analogous to the Russian grade 08Cr18Ni10), obtained by laser alloying in a powder bed and subjected to UNSM, on the basis of temperature-independent plasticity models. The authors of this work found that plastic deformation occurs only when the tip velocity and energy, as well as the applied stress, exceed a critical value corresponding to the yield strength of 08Cr18Ni10 steel, which changes dynamically with the increase of the processing time. It is worth noting that the strain energy accumulated in the dislocations is an additional factor contributing to the martensitic transformation [32].

Despite the fact that only a fraction of the total amount of strain energy is spent on the formation of martensite, the nucleation of which occurs predominantly at the intersection of shear bands [33], the nature of the  $V\alpha' = f(E)$  dependence can be analyzed as follows. On the one hand, there is a phenomenological relationship between the value of the stored energy (strain energy) and the flow stress of various steels and alloys (including 18-10 ASS), which has a quadratic character  $E \sim \sigma^2$  [29]. On the other hand, it has been established by experimental and computational methods that the volume fraction of martensite in strain-affected AISI 301LN (X2CrNi18-7 according to DIN) [34] and AISI 304L (Russian analog 03Cr18Ni11) [32] steels is proportional to the square of the flow stress ( $V\alpha' \sim \sigma^2$ ) under conditions of significant applied stresses. Thus, the dependence, shown in Fig. 2a, between the martensite volume fraction in the near-

surface layer of AISI 321 steel and the energy density of its deformation by UNSM satisfies the relationship  $V\alpha' \sim E$ .

It is important to note that the linear correlation  $V\alpha' \sim \sigma^2$  is not fulfilled in the whole range of values of the volume fraction of the martensitic phase, but under the condition of DIM is formed in the amount exceeding 30%. An original interpretation of this effect based on the percolation theory is proposed in Talonen et al. [34] and Bönisch et al. [35]. The value of the volume fraction of deformation-induced martensite  $V\alpha' = 0.3$  is considered as a certain critical value corresponding to the percolation threshold of the martensitic phase, which is 0.312 [34]. The authors associate the exceeding of this threshold with the formation of a certain “unitary cluster” (continuous network of martensitic phase) distributed throughout the deformed ASS volume. At this stage of plastic deformation of metastable austenitic stainless steels, the hardening effect becomes more pronounced due to the simultaneous deformation of both austenitic and martensitic phases, accompanied by an increase in the volume fraction of deformation-induced martensite [35].

As can be seen from the experimental data obtained in this work, all values of the volume fraction of DIM in the near-surface layer of AISI 321 steel after UNSM belong to the range  $V\alpha' > 0.3$  and form a directly proportional dependence of the form  $f(V\alpha') = 24.04E + 19.92$ . In turn, the strain energy density is in a linear relationship with the surface processing density  $N$  (see formula (2) in the Materials and Methods section), which causes the  $V\alpha' = f(N)$  dependence to be approximated by a similar first-order regression equation  $f(V\alpha') = 0.006N + 19.92$  as shown in Fig. 2b.

At the same time, Li et al. [22] and Wang et al. [23] report on the nonlinear nature of the relationship between the volume fraction of DIM and the surface processing density (impact intensity or number of passes) of 18-10 ASS by UIT, while the experimental data are not approximated by a functional dependencies. A monotonic growth in the deformation-induced martensite volume fraction from 8.7 to 13.6% and up to 17.2% occurs with the increase in the surface processing density of UIT from 40000 to 57600 and then up to 75000  $\text{mm}^{-2}$ , which contributes to a significant enhancement in the wear resistance and hardness of coatings formed by gas arc cladding of stainless steel (~15.5% chromium and ~8% nickel) [22].

Ultrasonic impact treatment of steel grade 08Cr18Ni10 at intensities of 3, 6 and 24  $\text{min}\cdot\text{cm}^{-2}$  provides an increase in the volume fraction of the martensitic phase from 83 to 96% and up to 100%, respectively, which has a nonlinear character and is accompanied by grain refinement and mechanical twinning [23]. In addition, the use of alternative methods of surface severe plastic deformation with varying processing density (coverage extent) also leads to a nonlinear change in the volume fraction of the martensitic phase. For example, in AISI 301 steel with austenite microstructure ( $V\alpha' < 3\%$  after annealing, in delivery condition) shot peened with coverage up to 200 and 400% and initial bead velocities of 65 and 75  $\text{m}\cdot\text{s}^{-1}$ , a nonlinear increase in the deformation-induced martensite volume fraction is observed, reaching ~30% relative to the corresponding initial value [36].

Thus, the authors of the above-mentioned works have studied the effect of ultrasonic impact and shot peening on the phase composition of 18-10 ASS, in which the volume fractions of the martensitic phase after processing in most cases either do not belong to the range  $V\alpha' > 0.3$  [22, 36] or are close to the saturation limit ( $83\% < V\alpha' \rightarrow 100\%$ ) [23]. In other words, there is no possibility to verify the experimental relation  $V\alpha' = f(N)$  obtained by means of a comparative analysis with the results of alternative studies.

The results of TEM-analysis (Fig. 3) at the qualitative level confirm the data obtained by XRD method on the structural-phase composition of the near-surface layer of AISI 321 steel, subjected to UNSM. It is worth noting that in Fig. 3a in the lower left corner a thin layer of platinum formed on the surface of the specimen during its preparation is visualized.

As the bright-field TEM image (Fig. 3a) and the corresponding microdiffraction (MD, Fig. 3b) pattern show, the structure of the near-surface layer of the specimen N1 after UNSM with a processing density of  $N = 9367 \text{ mm}^{-2}$  is biphasic ( $\alpha' + \gamma$ ) with a predominant content of DIM. Figure 3b is an alternation of rings corresponding to the martensitic phase, however, weak austenitic reflexes  $g = [200]\gamma$  are also present in the MD pattern. The TEM image (Fig. 3a) shows elongated martensitic lamellae with widths not exceeding 100 nm, oriented mainly parallel to the specimen surface, as well as a martensite dislocation structure with a high dislocation density of  $\sim 10^{15} \text{ m}^{-2}$ .

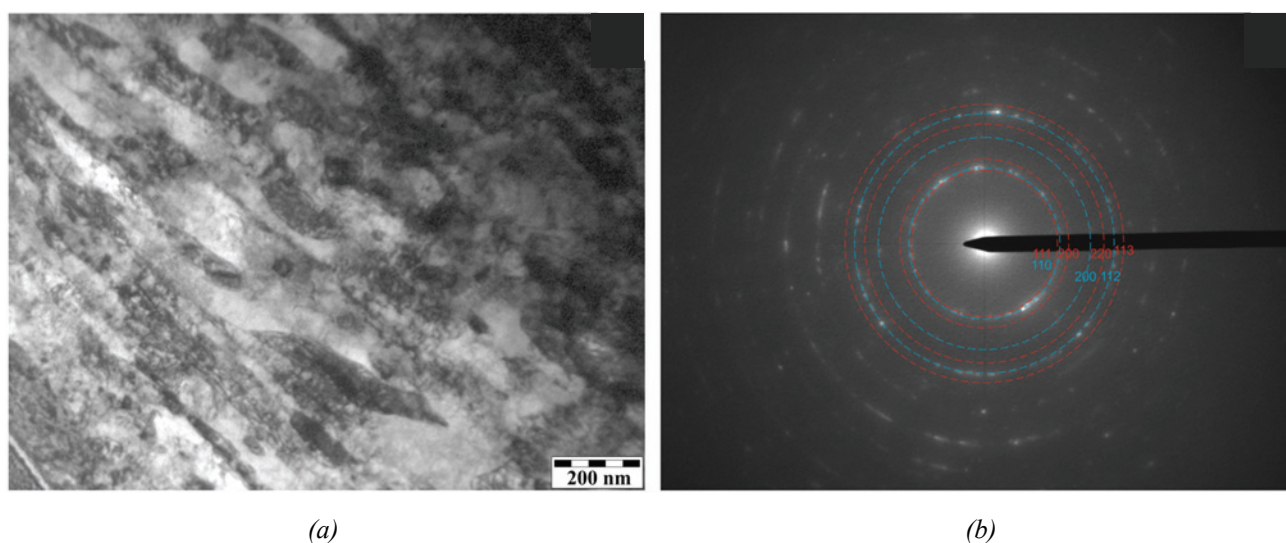


**Fig. 3.** Near-surface layer's structure of AISI 321 stainless steel after UNSM with  $N = 9367 \text{ mm}^{-2}$  processing density (specimen #1): (a) is TEM bright-field image of a cross-section parallel to the processing direction; (b) is the corresponding micro diffraction pattern with the reflections of  $\alpha'$ - and  $\gamma$ -phases

Accordingly, as a result of SSPD by ultrasonic nanocrystal surface modification, a two-phase ( $\alpha' + \gamma$ ) nanostructure is formed in the near-surface layer of AISI 321 steel. Thus, UNSM with the processing density  $N = 9367 \text{ mm}^{-2}$  provides the formation in the surface layer of AISI 321 steel of a structural state characterized by a high content of deformation-induced martensite in the form of nano-sized lamellae (strips) and a developed dislocation structure.

#### 4. Conclusion

During the experimental study of the phase composition of the near-surface layer of AISI 321 steel, a linear correlation between the volume fraction of martensite phase ( $V_{\alpha'}$ ), strain energy ( $E$ ) and processing density ( $N$ ) was established by the UNSM method. Approximation of the corresponding dependencies by first order regression equations  $f(V_{\alpha'}) = 24.04E + 19.92$  and  $f(V_{\alpha'}) = 0.006N + 19.92$  in the range of  $V_{\alpha'} \cong (30 \div 80) \%$  values is performed with reliability  $R^2 = 0.984$ . The interpretation of the obtained results is carried out using the concept of “percolation threshold”, as well as on the basis of phenomenological relationships between the yield stress and the strain energy, as well as with the volume fraction of the martensitic phase.

The results of TEM analysis at the qualitative level confirm the data obtained by XRD on the two-phase ( $\alpha' + \gamma$ ) composition of AISI 321 steel subjected to ultrasonic nanocrystal surface modification. UNSM with processing density  $N = 9367 \text{ mm}^{-2}$  provides structural transformation of the near-surface layer of AISI 321 steel containing a significant amount of deformation-induced martensite in the form of lamellae with width less than 100 nm and developed dislocation structure.

The obtained results can be used for improvement of physical-mechanical and functional properties, as well as for optimization of technological and operational characteristics of products made of 18-10 ASS using traditional subtractive, additive and hybrid additive-subtractive production technologies.

#### 5. Funding

This study received no external funding.

#### 6. Acknowledgements

The authors of the article express their gratitude to the staff of the Nanotech Research Center of the Federal State Budgetary Institution of Science “Institute of Strength Physics and Materials Science,

Siberian Branch of the Russian Academy of Sciences” (ISPMS SB RAS, Tomsk) and personally to Dr. I. Litovchenko for conducting the research and assistance in interpreting the results obtained by transmission electron microscopy.

#### 7. Conflict of interests

The authors declare no conflict of interests.

#### References

1. Beck T, Smaga M, Antonyuk S, Eifler D, et al. *Influence of Manufacturing and Load Conditions on the Phase Transformation and Fatigue of Austenitic Stainless Steels*. Cham: Springer; 2023. p. 257-288. DOI:10.1007/978-3-031-35575-2\_11
2. Qiu Y, Yang H, Tong L, Wang L. Research progress of cryogenic materials for storage and transportation of liquid hydrogen. *Metals*. 2021;11(7):1101-1114. DOI:10.3390/met11071101
3. Shalaby HM. Failure investigation of 321 stainless steel pipe to flange weld joint. *Engineering Failure Analysis*. 2017;80:290-298. DOI:10.1016/j.engfailanal.2017.06.047
4. Min KS, Kim KJ, Nam SW. Investigation of the effect of the types and densities of grain boundary carbides on grain boundary cavitation resistance of AISI 321 stainless steel under creep-fatigue interaction. *Journal of Alloys and Compounds*. 2004;370(1-2):223-229. DOI:10.1016/j.jallcom.2003.09.129
5. Titouche N-E, Boukharouba T, Amzert SA, Hassan AJ, et al. Direct drive friction welding effect on mechanical and electrochemical characteristics of titanium stabilized austenitic stainless steel (AISI 321) research reactor thick tube. *Journal of Manufacturing Processes*. 2019;41:273-283. DOI:10.1016/j.jmapro.2019.03.016
6. Gurovich BA, Kuleshova EA, Frolov AS, Maltsev DA, et al. Investigation of high temperature annealing effectiveness for recovery of radiation-induced structural changes and properties of 18Cr-10Ni-Ti austenitic stainless steels. *Journal of Nuclear Materials*. 2015;465:565-581. DOI:10.1016/j.jnucmat.2015.06.045
7. Acharya S, Suwas S, Chatterjee K. Review of recent developments in surface nanocrystallization of metallic biomaterials. *Nanoscale*. 2021;13(4):2286-2301. DOI:10.1039/D0NR07566C
8. Laleh M, Sadeghi E, Revilla RI, Chao Q, et al. Heat treatment for metal additive manufacturing. *Progress in Materials Science*. 2023;133:101051. DOI:10.1016/j.pmatsci.2022.101051
9. Wang X, Hu Q, Liu W, Yuan W, et al. Microstructure and corrosion properties of wire arc additively manufactured multi-trace and multilayer stainless steel 321. *Metals*. 2022;12(6):1039. DOI:10.3390/met12061039
10. Ma G, Li L, Chen Y. Effects of beam configurations on wire melting and transfer behaviors in dual beam laser welding with filler wire. *Optics & Laser Technology*. 2017;91:138-148. DOI:10.1016/j.optlastec.2016.12.019

11. Moskvina VA, Melnikov EV, Astafurov SV, Panchenko MYu, et al. Stable high-nickel austenitic steel produced by electron beam additive manufacturing using dual wire-feed system. *Materials Letters*. 2021;305:130863. DOI:10.1016/j.matlet.2021.130863
12. Osipovich K, Kalashnikov K, Chumaevskii A, Gurianov D, et al. Wire-feed electron beam additive manufacturing: A review. *Metals*. 2023;13(2):279. DOI:10.3390/met13020279
13. Zhou C, Jiang F, Xu D, Guo C, et al. A calculation model to predict the impact stress field and depth of plastic deformation zone of additive manufactured parts in the process of ultrasonic impact treatment. *Journal of Materials Processing Technology*. 2020;280:116599. DOI:10.1016/j.jmatprotec.2020.116599
14. Tiamiyu AA, Eduok U, Szpunar JA, Odeshi AG. Corrosion behavior of metastable AISI 321 austenitic stainless steel: investigating the effect of grain size and prior plastic deformation on its degradation pattern in saline media. *Scientific Reports*. 2019;9(1):12116. DOI:10.1038/s41598-019-48594-3
15. Ye C, Zhang C, Zhao J, Dong Y. Effects of post-processing on the surface finish, porosity, residual stresses, and fatigue performance of additive manufactured metals: a review. *Journal of Materials Engineering and Performance*. 2021;30(9):6407-6425. DOI:10.1007/s11665-021-06021-7
16. Shi X, Xiao Z, Wu J. *The use of nanotechnology to improve the bulk and surface properties of steel for structural applications*. In: Nanotechnology in Eco-Efficient Construction. Cambridge: Woodhead Publishing Ltd; 2013. p. 75-107. DOI:10.1533/9780857098832.1.75.
17. Cao Y, Ni S, Liao X, Song M, et al. Structural evolutions of metallic materials processed by severe plastic deformation. *Materials Science and Engineering: R: Reports*. 2018;133:1-59. DOI:10.1016/j.mser.2018.06.001
18. Wu B, Zhang J, Zhang L, Pyoun Y-S, et al. Effect of ultrasonic nanocrystal surface modification on surface and fatigue properties of quenching and tempering S45C steel. *Applied Surface Science*. 2014;321:318-330. DOI:10.1016/j.apsusc.2014.09.068
19. Kishore A, John M, Ralls AM, Jose SA, et al. Ultrasonic nanocrystal surface modification: processes, characterization, properties, and applications. *Nanomaterials*. 2022;12(9):1415. DOI:10.3390/nano12091415
20. Yuan Y, Li R, Bi X, Yan M, et al. Review on numerical simulation of ultrasonic impact treatment (UIT): Present situation and prospect. *Journal of Materials Research and Technology*. 2024;30:1319-1340. DOI:10.1016/j.jmrt.2024.03.107
21. Kim C, Park S, Pyoun Y, Shim D. Effects of ultrasonic nanocrystal surface modification on mechanical properties of AISI D2 steel. *International Journal of Precision Engineering and Manufacturing*. 2021;22(7):1271-1284. DOI:10.1007/s12541-021-00536-8
22. Li L, Guo S, Jia L, Zhang L, et al. Enhanced wear behavior of a stainless steel coating deposited on a medium-carbon low-alloy steel using ultrasonic impact treatment. *Coatings*. 2023;13(12):2024. DOI:10.3390/coatings13122024
23. Wang GQ, Lei MK, Guo DM. Interactions between surface integrity parameters on AISI 304 austenitic stainless steel components by ultrasonic impact treatment. *Procedia CIRP*. 2016;45:323-326. DOI:10.1016/j.procir.2016.02.351
24. Sun L, Huang L, Wu P, Huang R, et al. Progress on the effect and mechanism of ultrasonic impact treatment on additive manufactured metal fabrications. *Crystals*. 2023;13(7):995. DOI:10.3390/cryst13070995
25. Kim MS, Park SH, Pyun YS, Shim DS. Optimization of ultrasonic nanocrystal surface modification for surface quality improvement of directed energy deposited stainless steel 316L. *Journal of Materials Research and Technology*. 2020;9(6):15102-15122. DOI:10.1016/j.jmrt.2020.10.092
26. Diao M, Guo C, Sun Q, Jiang F, et al. Improving mechanical properties of austenitic stainless steel by the grain refinement in wire and arc additive manufacturing assisted with ultrasonic impact treatment. *Materials Science and Engineering: A*. 2022;857:144044. DOI:10.1016/j.msea.2022.144044
27. Polonyankin DA, Fedorov AA, Blesman AI, Nesov SN. Structural coloration of AISI 321 steel surfaces textured by ultrasonic impact treatment. *Optics & Laser Technology*. 2022;150:107948. DOI:10.1016/j.optlastec.2022.107948
28. Li L, Kim M, Lee S, Bae M, et al. Influence of multiple ultrasonic impact treatments on surface roughness and wear performance of SUS301 steel. *Surface and Coatings Technology*. 2016;307:517-524. DOI:10.1016/j.surfcoat.2016.09.023
29. Sendrowicz A, Myhre AO, Yasnikov IS, Vinogradov A. Stored and dissipated energy of plastic deformation revisited from the viewpoint of dislocation kinetics modelling approach. *Acta Materialia*. 2022;237:118190. DOI:10.1016/j.actamat.2022.118190
30. Xia P, Canillas Rodríguez FJ, Sabirov I. Microstructure evolution and adiabatic heating during dynamic biaxial deformation of a 304 stainless steel. *Materials Science and Engineering: A*. 2020;793:139829. DOI:10.1016/j.msea.2020.139829
31. Zhou C, Wang J, Guo C, Zhao C, et al. Numerical study of the ultrasonic impact on additive manufactured parts. *International Journal of Mechanical Sciences*. 2021;197:106334. DOI:10.1016/j.ijmecsci.2021.106334
32. Fang XF, Dahl W. Strain hardening and transformation mechanism of deformation-induced martensite transformation in metastable austenitic stainless steels. *Materials Science and Engineering: A*. 1991;141(2):189-198. DOI:10.1016/0921-5093(91)90769-J
33. Ahmedabadi PM, Kain V, Agrawal A. Modelling kinetics of strain-induced martensite transformation during plastic deformation of austenitic stainless steel. *Materials & Design*. 2016;109:466-475. DOI:10.1016/j.matdes.2016.07.106
34. Talonen J, Hänninen H, Nenonen P, Pape G. Effect of strain rate on the strain-induced  $\gamma \rightarrow \alpha'$ -

martensite transformation and mechanical properties of austenitic stainless steels. *Metallurgical and Materials Transactions A*. 2005;36(2):421-432. DOI:10.1007/s11661-005-0313-y

35. Bönisch M, Barriobero-Vila P, Dhekne PP, Stark A, et al. Tension-compression asymmetry of metastable austenitic stainless steel studied by in-situ high-

energy X-ray diffraction. *International Journal of Plasticity*. 2023;170:103767. DOI:10.1016/j.ijplas.2023.103767

36. Fargas G, Roa JJ, Mateo A. Effect of shot peening on metastable austenitic stainless steels. *Materials Science and Engineering: A*. 2015;641:290-296. DOI:10.1016/j.msea.2015.05.079

### Information about the authors / Информация об авторах

**Denis A. Polonyankin**, Cand. Sc. (Pedagogy), Associate Professor, Omsk State Technical University (OmSTU), Omsk, Russian Federation; ORCID 0000-0001-6799-3105; e-mail: dapolonyankin@omgtu.tech

**Alexey A. Fedorov**, Cand. Sc. (Tech.), Associate Professor, OmSTU, Omsk, Russian Federation; ORCID 0000-0002-6681-087X; e-mail: aafedorov@omgtu.ru

**Tatyana M. Gomonyuk**, Design Engineer, CJSC “Elekton”, Raduzhny, Russian Federation; Postgraduate Student, OmSTU, Omsk, Russian Federation; ORCID 0000-0002-6703-0242; e-mail: gomonyuk1998@mail.ru

**Полонянкин Денис Андреевич**, кандидат педагогических наук, доцент, Омский государственный технический университет (ОмГТУ), Омск, Российская Федерация; ORCID 0000-0001-6799-3105; e-mail: dapolonyankin@omgtu.tech

**Федоров Алексей Аркадьевич**, кандидат технических наук, ОмГТУ, Омск, Российская Федерация; ORCID 0000-0002-6681-087X; e-mail: aafedorov@omgtu.ru

**Гомонок Татьяна Михайловна**, инженер-конструктор, ЗАО «Электон», Радужный, Российская Федерация; аспирант, ОмГТУ, Омск, Российская Федерация; ORCID 0000-0002-6703-0242; e-mail: gomonyuk1998@mail.ru

*Received 03 September 2024; Accepted 07 October 2024; Published 20 December 2024*



**Copyright:** © Polonyankin DA, Fedorov AA, Gomonyuk TM, 2024. This article is an open access article distributed under the terms and conditions of the Creative Commons Attribution (CC BY) license (<https://creativecommons.org/licenses/by/4.0/>).